Pump-Wavelength Dependence of Raman Gain in Single-Mode Optical Fibers

Nathan R. Newbury

***Abstract*—The magnitude of the stimulated Raman gain spectrum depends on the absolute wavelength of the pump laser. For many fibers, this dependence can be cast as a simple scaling of the overall gain curve according to a power-law dependence on the pump wavelength. We present three methods of measuring this scaling: estimation from Raman gain theory and known fiber parameters, a brute-force comparison of gain versus pump wavelength, and a more elegant comparison of the asymmetry in the Stokes and anti-Stokes Raman gain spectrum at a fixed pump wavelength. We discuss the advantages of the asymmetry technique, which yields the full wavelength dependence of the Raman gain with low uncertainty using only a single pump laser, a broadband source, and an optical spectrum analyzer. Finally, we report on the pump-wavelength scaling of the Raman gain for a number of standard transmission fibers.**

***Index Terms*—Optical fiber devices, Raman scattering.**

I. Introduction

In a fiber Raman amplifier, a strong pump laser provides gain to signals at longer wavelengths through stimulated Raman scattering [1]–[5]. At typical pump wavelengths of 1.3–1.5 μm, the Raman scattering in optical fiber occurs far from any electronic resonance, so that the gain depends strongly on the difference between the pump and signal wavelengths and only weakly on the absolute wavelength of either the pump or signal beams. Indeed, one of the major attractions of Raman amplification is that it can be used over a very wide wavelength range by multiplexing together different pump wavelengths [6], [7]. Initial measurements of the Raman gain focused on the strong dependence of the gain on the pump-signal wavelength difference [8]–[13], and understandably ignored the weaker dependence of the gain on the absolute pump wavelength. However, with the growing importance of Raman amplifiers [14]–[16], knowledge of the dependence of Raman gain on the absolute pump wavelength is equally important. It can be used to predict the Raman gain at an arbitrary pump wavelength, it can help in simulating the gain response of an amplifier that employs a number of different pump wavelengths, and it can assist in predicting the effect of Raman gain tilt in dense wavelength-division multiplexing (WDM) systems.

In [17], this author published the first measurements of pump-wavelength scaling of Raman gain using two different complementary techniques: a gain-asymmetry technique and a gain-comparison technique. In total, the author has demonstrated four methods for determining the pump-wavelength scaling of the Raman gain. The first, "gain comparison," relies on a comparison of gain curves measured with different pump lasers. The second, "gain asymmetry," relies on a comparison of the Stokes and anti-Stokes sides of the Raman gain curve to extract the pump-wavelength dependence. The third method is a variant of the gain-asymmetry technique in which the pump-wavelength scaling is extracted from the asymmetry in the spontaneous Raman scattering spectrum [18]. This method relies on the direct relation of the spontaneous Raman scattering spectrum to the stimulated Raman gain spectrum, which is a consequence of the simple harmonic energy levels of the glass vibrational modes. The fourth method relies on a combination of the well-known theory for Raman gain and previously measured fiber parameters to estimate the pump-wavelength scaling [19]. This method takes advantage of the fact that the pump-wavelength scaling is effectively dominated by the wavelength scaling of the effective area of the fiber.

In this paper, we present and compare measurements of the pump-wavelength scaling of the Raman gain for a number of standard transmission fibers using estimations based on known fiber parameters, the gain-comparison method, and the gain-asymmetry method. (We do not explicitly discuss extracting the pump-wavelength scaling from the spontaneous Raman gain curve, since that method was treated in detail in [18] and typically has an accuracy lower than that of the stimulated gain-asymmetry method discussed here.) While the emphasis of this paper is on the pump-wavelength scaling, all of the experimental methods actually provide the *full* wavelength dependence of the Raman gain since they also yield the dependence of the Raman gain on the pump-signal wavelength difference. For standard fibers, the simple picture of a pump-wavelength scaling of the overall Raman gain curve works very well over the wavelength range of interest. However, for dispersion-compensating fibers (DCFs), this simple picture appears to break down, and an accurate description of the Raman gain requires a direct measurement at or near the pump wavelength of interest.

The gain-asymmetry method, first introduced by the author in [17], is by far the simplest method and has by far the lowest uncertainty. It has a number of distinct advantages over the other methods. First, it requires only a single pump laser, as opposed to the more brute-force gain-comparison technique that requires at least two pump lasers. Second, it is a direct measurement of the pump-wavelength scaling. Third, it is completely independent of the absolute or even relative pump power and signal power and is therefore free of the otherwise potentially limiting systematic uncertainties associated with any power measurements. Fourth, the typical uncertainty in the pump-wavelength

Manuscript received March 31, 2003; revised September 2, 2003.

The author is with the National Institute of Standards and Technology, Boulder, CO 80305 USA (e-mail: nnewbury@ boulder.nist.gov).

Digital Object Identifier 10.1109/JLT.2003.821716

scaling is ∼2–10 times smaller than with the gain-comparison method. Finally, and most importantly, its implementation is a relatively straightforward extension of the typical experimental setup used to measure the Raman gain spectrum. Because [17] focused on a comparison of the two techniques, a low-power pump was used, necessitating a complicated detection system. Here the author demonstrates that if only the asymmetry technique is used to measure the pump-wavelength dependence, a much simpler experimental apparatus can be used. Indeed, the same setup and data may be used to simultaneously determine the Raman gain dependence on both the signal-pump wavelength difference and the absolute pump wavelength.

Section II below briefly overviews the theory of Raman gain [2], [3], [5], with particular emphasis on the pump-wavelength scaling. Section III gives estimates of the pump-wavelength scaling based on the theory and the known fiber parameters (in particular the wavelength-dependence of the effective area). The discussions of the gain-asymmetry and gain-comparison methods are combined in the next sections since they are based on the same data set. Specifically, Section IV describes two different experimental setups used in both the gain-asymmetry and gain-comparison measurements of the pump-wavelength scaling and Section V describes the results of the gain-asymmetry and gain-comparison methods. Section V also gives an overall comparison of the results for all three methods for the various fibers measured and provides values for the pump-wavelength scaling for several standard transmission fibers. Section VI briefly discusses the combined effects of the pump-wavelength dependence of the Raman gain coefficient and of the fiber attenuation on the overall wavelength dependence of a distributed amplifier.

II. Theory

Before writing explicit expressions for the Raman gain, it is instructive to consider the basic properties of the Raman gain coefficient that result from conservation of photon number. As is shown below, the gain-asymmetry method relies only on photon number conservation and some explicit assumptions about the separability of the Raman gain.

Stimulated Raman transitions in a fiber will convert pump photons at frequency ω_p to signal photons at frequency ω_s. At nonzero temperatures, *spontaneous* Raman scattering can cause conversion of the pump photons to signal photons at either higher or lower frequencies with a temperature-dependent spectrum [12], [18], [20], [21]; however, the *stimulated* Raman transitions considered here will always result in the conversion of a higher frequency photon into a lower frequency photon. In Raman amplifiers, the "pump" beam is assumed to refer to the beam with both the most power and the highest frequency, so that the weaker signal beam is amplified. For the argument below, we will likewise assume that the pump beam is much stronger than the signal in order to make the simplifying assumption of an "undepleted" pump; however, here we let the signal frequency be either lower (Stokes side) or higher (anti-Stokes side) than the pump frequency. If $R(\omega_s,\omega_p)$ is the stimulated Raman transition rate for conversion of pump photons to signal photons when $\omega_s < \omega_p$, then it must be true that $R(\omega_p,\omega_s)$ is the stimulated Raman transition rate for conversion of signal photons to pump photons when $\omega_p < \omega_s$. In a single-mode fiber, the rate R will be spatially dependent, and the gain (or loss) of power in the signal beam P_s at a pump power P_p will be given by

$$\begin{aligned}\frac{dP_s}{dz} &= +\hbar\omega_s \int R(\omega_s,\omega_p)dxdy \\ &\equiv g^+(\omega_p,\Delta\omega)P_sP_p \quad \Delta\omega > 0 \\ \frac{dP_s}{dz} &= -\hbar\omega_s \int R(\omega_p,\omega_s)dxdy \\ &\equiv g^-(\omega_p,\Delta\omega)P_sP_p \quad \Delta\omega < 0 \end{aligned} \tag{1}$$

where z is the propagation direction down the assumed single-mode fiber $\Delta\omega = \omega_p - \omega_s$ and $g^+(g^-)$ is the wavelength-dependent modal Raman gain (loss) coefficient for $\omega_s < \omega_p\,(\omega_s > \omega_p)$. (In writing (1), we have assumed that the stimulated rate is proportional to both the signal and pump power). The gain $g^{+(-)}$ is of course identically zero for $\Delta\omega = 0$, so that the gain g is continuous across zero frequency offset and the $\pm$ superscript is technically not needed; however, it is useful to retain the superscript in the later discussion of the pump-wavelength scaling. From (1), it is clear that the stimulated Raman gain for a pump at, for example, 1450 nm and a signal at 1500 nm is just (1450/1500) times the stimulated loss for a pump at 1500 nm and a signal at 1450 nm.

To go further in extracting the pump-wavelength scaling from the full Raman gain spectrum requires an additional assumption that the dominant effect of changing the pump wavelength is an overall change of scale in the Raman gain spectrum; the actual shape of the Raman gain spectrum is assumed to remain the same. In other words, the modal Raman gain coefficient is written as a separable product of a slowly varying functionof the pump frequency and a rapidly varying function ρ that depends only on the frequency difference $\Delta\omega = \omega_p - \omega_s$. This assumption is actually implicit in even discussing a pump-wavelength "scaling" of the Raman gain curve and, as is shown later, is valid for most standard transmission fibers, with the exception of DCF. Mathematically, the assumption is that

$$g^+(\omega_p,\Delta\omega) \approx f(\omega_p)\,\rho(\Delta\omega)\,C \tag{2}$$

where f is the function that describes the pump-wavelength scaling of the Raman gain and C is a frequency-independent constant evaluated at the reference pump frequency. In that case, from (1)

$$g^-(\omega_p,\Delta\omega) \approx -\frac{\omega_s}{\omega_p} f(\omega_s)\,\rho(-\Delta\omega)\,C. \tag{3}$$

The variation of the function f can be found based on the asymmetry (or alternatively the ratio) of the gain versus the loss about the pump frequency, which is

$$\begin{aligned} A(\Delta\omega) &= \frac{g^+(\omega_p,\Delta\omega) + g^-(\omega_p,-\Delta\omega)}{g^+(\omega_p,\Delta\omega,) - g^-(\omega_p,-\Delta\omega)} \\ &\approx -\left[\frac{d\ln f}{2d\omega_p} + \frac{1}{2\omega_p}\right]\Delta\omega \end{aligned} \tag{4}$$

to first order in $\Delta\omega/\omega_p$. The functional form of f is undetermined; following [17] for simplicity, we choose to describe the function f by its leading power-law behavior

$$f \sim \omega_p^{n_s} \tag{5}$$

where the exponent n_s describes the power-law scaling of the Raman gain with the pump wavelength. The value of this power-law exponent is directly related to the asymmetry and is given, after substitution of (5) into (4), by

$$A(\Delta\omega) = -\frac{n_s+1}{2\omega_p}\Delta\omega. \tag{6}$$

In other words, the asymmetry in the gain spectrum, plotted as a function of $\Delta\omega$, should be a straight line with a slope that gives the exponent of the power-law scaling. Over a wider range of wavelengths, the simple power-law scaling can be modified by including the wavelength dependence of the exponent; this wavelength dependence is in fact measured in the data set presented below. Note that the function f could have been written instead as a function of ω_s, or of both ω_s and ω_p, without changing the results.

Equations (5) and (6) are the basis for the gain-asymmetry technique of determining the power-law scaling. They were derived without any explicit assumptions about the form of the stimulated Raman scattering, other than the fact that it can be written as a separable function (2). Nevertheless, it is useful to consider the form of the stimulated Raman transition rate to gain some insight into the different factors responsible for the wavelength scaling of the Raman gain. From second-order perturbation theory, the stimulated Raman transition rate due to applied electric fields $\mathbf{E}_1$ at frequency ω_1 and $\mathbf{E}_2$ at frequency $\omega_2 > \omega_1$ is

$$R(\omega_1,\omega_2) = \frac{2\pi}{\hbar^4}E_1^2(x,y)E_2^2(x,y)M^2N\rho(\omega_2-\omega_1) \tag{7}$$

where N is the density of participating molecules and $\rho(\omega_2-\omega_1)$ is the density of vibrational molecular states. The square of the matrix element M^2 determines the strength of the Raman interaction. For an initial state $|i\rangle$, assumed to be one of the ground vibrational states, and a final state $|f\rangle$, also in the ground-state vibrational manifold, the matrix element is given by the sum over virtual intermediate electronic states $|m\rangle$ as

$$M^2(\omega_1,\omega_2) = \left|\sum_m \frac{d_{fm}d_{mi}}{\omega_m+\omega_1} + \frac{d_{fm}d_{mi}}{\omega_m-\omega_2}\right|^2 \times \left(\frac{1}{2}\right). \tag{8}$$

Since the medium is isotropic and the gain is known to be significant only for parallel electric-field vectors, we have simplified the matrix element tensor by writing it in terms of the scalar matrix elements $d_{mi} = \langle m|d_x|i\rangle$, where d_x is one component of the vector dipole operator. The factor of one-half was introduced under the assumption that we are interested in the *unpolarized* Raman gain, where the relative polarization of the pump and probe is zero. At finite temperatures, this expression remains valid provided that the energy levels of the vibrational states follow those of a simple harmonic oscillator [18].

The presence of dopants in the core of the single-mode fiber will cause both the strength of the matrix element and the density of states to vary with position [22]–[24]. However, the effect of these variations on the pump-wavelength scaling is weak (see estimates below), and for our purposes those two factors can be taken out of the area integral (1). In that case, using the definition of the effective area [5]

$$A_{\text{eff}}(\omega_1,\omega_2) \equiv \frac{\int E_1^2(x,y)\,dxdy \int E_2^2(x,y)\,dxdy}{\int E_1^2(x,y)\,E_2^2(x,y)\,dxdy} \tag{9}$$

the modal Raman gain for the Stokes gain is given by

$$g^+ = \frac{8\pi^3 N}{c^2}\left[\frac{\omega_s M^2(\omega_s,\omega_p)}{n(\omega_s)\,n(\omega_p)\,A_{\text{eff}}(\omega_s,\omega_p)}\right]\rho(\Delta\omega). \tag{10}$$

A similar argument gives the modal Raman "gain" term describing the loss in power of the signal beam for $\Delta\omega < 0$ as

$$g^- = -\frac{8\pi^3 N}{c^2}\left[\frac{\omega_s M^2(\omega_p,\omega_s)}{n(\omega_p)\,n(\omega_s)\,A_{\text{eff}}(\omega_p,\omega_s)}\right]\rho(-\Delta\omega) \tag{11}$$

where $n(\omega)$ is the index of refraction. Since the denominator is symmetric with exchange of the pump and signal frequencies, the only difference between the Stokes and anti-Stokes Raman gain factor is the interchange of the arguments of the matrix element and of the sign of $\Delta\omega$, as had to be the case based on (1). A common assumption in the literature is that the product gA_{eff} scales as the inverse pump wavelength. In fact, it is clear from (10) that it actually scales as the inverse *signal* wavelength (ignoring the dependence of the matrix element or index of refraction). However, since the signal and pump wavelengths typically differ by less than 100 nm in the infrared (IR), the resulting error is $\leq$1%.

III. Estimating the Pump-Wavelength Scaling From Theory and Measured Fiber Parameters

The term in square brackets in (10) or (11) contains the factors that contribute to the wavelength scaling of the Raman gain. In general, it is important to note from (10) that the Raman gain is, in fact, not separable in terms of $\Delta\omega$ and ω_p, indicating that there is no simple universal pump-wavelength scaling. However, a simple power-law scaling can often adequately describe the wavelength scaling of the modal Raman gain over the wavelength of interest, which for our purposes is ~1.3–1.7 μm in single-mode fiber. To identify the factors responsible for this power-law scaling, we can determine the leading power-law behavior of each of the contributing terms in (10) following [19].

The dependence of the first factor of ω_s, which arises from converting the Raman scattering rate into a rate of power transfer, is easily approximated as $\omega_s \approx \omega_p$ plus terms of order $\Delta\omega/\omega_p$.

The dependence of the second factor of M^2/n^2 on ω_p can also be estimated. Since the matrix element $M^2(\omega,\omega) \propto \left(n^2(\omega)-1\right)^2$, the Sellmeier equations can be used to yield $M^2/n^2 \approx \omega_p^{0.07}$ over the wavelength range of 1–2 μm[19], [25]. The exact power-law dependence will of course depend on the glass dopants, but will not vary substantially. Note that this term has been used to explain the discrepancy between Raman gain curves measured in the visible and the IR [25].

The final contributor to the power-law scaling is the effective area. Unfortunately, the dependence of the effective area on the pump frequency is challenging to estimate. We explicitly write the leading power-law dependence as $A_{\text{eff}}(\omega_p, \omega_s) = \omega_p^{-n_A}$. It is tempting to then rewrite the effective area as $A_{\text{eff}}(\omega_p, \omega_s) = k\pi\left[r_0^2(\omega_p) + r_0^2(\omega_s)\right]/2$, where r_0 is the standard Gaussian beam width parameter describing the fiber mode. However, such an approach is not accurate enough to capture the true wavelength dependence of the effective area for two reasons. First, the constant k is itself wavelength dependent [26], and second, any wavelength-dependent errors in the estimation of the Gaussian beamwidth lead to large errors in the wavelength dependence of the effective area. For example, an error of only ~2% in r_0 over the range of 1.3–1.5 μm leads to an error in the exponent n_A of 0.3. Clearly, for nonstep index fibers at least, a detailed knowledge of the index profile is needed to accurately calculate the effective area. However, even for a nominal "step index" fiber such as SMF-28, it is difficult to estimate the wavelength dependence. Using a nominal cutoff wavelength of 1.26 μm, the standard Gaussian beam approximation yields a wavelength dependence at 1.43 μm of $n_A = 1.6$. Calculating the effective area with the true Bessel functions of the fundamental mode gives a very different value of $n_A = 1.45$, but even this value will depend on the actual cutoff wavelength and, presumably, how sharply the index profile changes at the "step." For example, reported measurements of the wavelength dependence at 1.43 μm show the actual value of n_A to be closer to 1.3 [27]. Therefore, accurate estimates of the power-law scaling of the effective area require accurate direct measurements of either the wavelength dependence of the effective area or the true index profile of the fiber.

As a final complication, the separation of the Raman gain in terms of a Raman matrix element and an effective area is only an approximation; the Raman matrix element and density-of-states factors will vary across the transverse fiber dimensions due to the same doping that raises the index to provide guiding of the light. Therefore, the variation in both factors should be included in the overlap integral that defines the effective area. Based on estimates of the variation in the Raman gain from Ge doping [22], including this variation in the overlap integral will increase the effective value of n_A by ~0.03 for a step index fiber.

Including all the factors, the power-law scaling of the Raman gain is given by

$$g^+ \approx \omega_p^{1+0.1+n_A}\rho(\Delta\omega)\,C \tag{12}$$

which is identical to (2) if the overall power-law scaling exponent of the Raman gain is identified as $n_s = 1.1 + n_A$. Based on this equation, given the scaling of the effective area with wavelength, one can estimate the scaling of the Raman gain with pump wavelength. In general, the challenges of measuring the wavelength scaling of the effective area are just as substantial as measuring the wavelength scaling of the Raman gain. Fortunately, however, Humphreys and coworkers have made a set of direct measurements of the effective area of relevant fibers at wavelengths of 1310 and 1550 nm using several different methods [27]. Using their data to estimate the power-law wavelength dependence of the effective area then yields the pump-wavelength scaling of the Raman gain from (12). The results are given in Table I. The quoted uncertainty assumes that the errors on the effective area measurements at different wavelengths are uncorrelated. An additional uncertainty of 0.1 was included

TABLE I
PUMP-WAVELENGTH SCALING OF RAMAN GAIN

Fiber Type	Gain Asymmetry	Gain Comparison	Estimate from Theory[d]
SMF-28 [a]	2.238 ± 0.097	1.91 ± 0.17	2.33 ± 0.11
SMF-28(e) [a]	2.277 ± 0.086	2.32 ± 0.17	2.33 ± 0.11
LEAF [a]	4.102 ± 0.085	4.29 ± 0.17	4.45 ± 0.12
TrueWave [a]	3.347 ± 0.080	3.40 ± 0.17	3.09 ± 0.11
SMF-28 [b]	2.319 ± 0.066		
SMF-28(e) [b]	2.356 ± 0.036		
LEAF [b]	4.201 ± 0.036		
TrueWave [b]	3.289 ± 0.082		
SMF-28 #2 [b]	2.322 ± 0.045	2.75 ± 0.68	2.33 ± 0.11
DC SM [b]	2.236 ± 0.045	2.40 ± 0.68	2.33 ± 0.11
LEAF #2 [b]	4.243 ± 0.071	3.93 ± 0.68	4.45 ± 0.12
TrueWave #2 [b]	3.282 ± 0.050	3.44 ± 0.68	3.09 ± 0.11
DCF [c]	6.3	5.8	

SMF-28 and LEAF fibers manufactured by Corning Inc. TrueWave and depressed cladding single-mode (DC SM) fibers manufactured by Lucent Technology. The use of product names is necessary to specify the experimental results adequately and does not imply endorsement by the National Institute of Standards and Technology.

All uncertainties represent one standard unit of uncertainty.

(a) Data taken using the setup of Fig. 2. The estimated power-law scaling exponent is for a pump wavelength of 1520 nm. The gain-asymmetry values are based on a linear fit similar to that shown in Fig. 7. The gain-comparison values are based on a linear fit similar to that shown in Fig. 6.

(b) Data taken using the setup of Fig. 1. The estimated power-law scaling exponent is for a pump wavelength of 1480 nm. The gain-asymmetry values are based on a single Raman gain spectrum taken at a pump wavelength of 1480 nm. The gain-comparison values are based on a two-point linear fit to the integrated gain measured at 1450 and 1480 nm.

(c) Values for the DCF fiber are given for comparison. However, no uncertainties are given since the assumption of a simple power-law scaling of the gain with pump-wavelength is demonstrably invalid. An approximate uncertainty might be ±1 for all values.

(d) The values were estimated using the wavelength dependence of the effective areas estimated from the data in [27], which are centered around 1430 nm. Correcting for the wavelength dependence of the exponent (see Table II) to a pump wavelength of 1500 would increase these values by ~0.1 to 0.2 depending on the fiber. The uncertainty is calculated as stated in Section III.

TABLE II
DEPENDENCE OF THE POWER-LAW EXPONENT (DESCRIBING THE PUMP-WAVELENGTH SCALING) ON THE PUMP WAVELENGTH

Fiber	$dn_s/d\lambda$ (nm^{-1})
SMF-28	0.0015 ± 0.0012
LEAF	0.0028 ± 0.0011
TrueWave	0.0037 ± 0.0009

to reflect the uncertainty of the matrix element and Ge doping contributions to the scaling. No additional uncertainties were included to account for the wavelength scaling of the exponent n_s or, perhaps most importantly, the fact that the fibers measured in [27] were not identical to the fibers used to measure the gain in this paper.

From (12), it is clear that the wavelength scaling of the effective area is the dominant contribution to the wavelength scaling of the Raman gain. Furthermore, the wavelength scaling of the effective area is also inherently connected with the dispersion characteristics of the fiber. As a result, dispersion-shifted fibers have a much stronger wavelength scaling than standard single-mode fibers. For fibers with very strong dispersion characteristics, such as DCF, the effective area appears to have such a complex wavelength dependence that the concept of a simple pump-wavelength scaling epitomized in (2) can break down.

IV. Gain-Asymmetry and Gain-Comparison Methods: Experimental Setup and Procedures

A. Introduction

We consider two possible experimental techniques to measure the wavelength dependence of the Raman gain: the gain-comparison method and the gain-asymmetry method, both of which were introduced in [17]. Additional measurements of the pump-wavelength dependence using the gain-comparison method were reported in [28]. In both the gain-comparison and gain-asymmetry method, a calibrated Raman gain spectrum at a specific pump wavelength is acquired to determine the Raman gain dependence on the pump-signal frequency difference. For the gain-asymmetry technique, this single calibrated Raman gain spectra *at one pump wavelength* is sufficient to determine the pump-wavelength scaling. For the gain-comparison technique, multiple such calibrated Raman gain spectra are needed at different pump wavelengths to determine the pump-wavelength dependence of the Raman gain. The experimental setup for either approach is similar; the difference between the two approaches lies in the number of different pump lasers required and the ultimate uncertainty in the pump-wavelength scaling, which is significantly smaller for the gain-asymmetry technique.

Depending on the available pump power, there are two possible experimental setups. If the pump power is sufficiently high, i.e., greater than 30 mW or so, the Raman gain will be high enough that a relatively simple experimental setup employing a standard optical spectrum analyzer (OSA) and broadband source is possible. If only a low pump power is available, then the Raman gain will be small, and a more sensitive detection system is required, as was the case in [17]. We discuss both experimental setups below with particular attention to the dominant sources of uncertainty. Again, either experimental setup can be used to generate the data needed by the gain-asymmetry or the gain-comparison method of measuring the pump-wavelength scaling of the Raman gain.

B. Experimental Setup for a High-Power Pump Laser

The experimental setup for a high-power pump laser, shown in Fig. 1, is essentially identical to that commonly used to determine the dependence of the Raman gain on just the pump-signal frequency difference [9], [29]. Several precautions are taken to avoid distorting the shape of the Raman gain spectrum. First, to avoid spurious Raman gain from amplified spontaneous emission (ASE) that might distort the spectrum at small pump-signal offsets, the pump diode is filtered by a Fabry–Perot filter, which removes the ASE and also reduces the linewidth to a root-mean-square width of 0.3 nm (still sufficiently broad to avoid any stimulated Brillouin scattering in the fiber [5]). To avoid polarization effects that might also distort the Raman gain shape [30], the polarization of the pump laser is scrambled to $<$10% and the signal light is likewise depolarized to $<$2%. The depolarization of the pump has the added benefit of reducing variations in pump power due to polarization-dependent loss of any optical components; the pump power is stable to better than 0.002 dB over a measurement period. To avoid transfer of the pump relative intensity noise to the signal probe [31], a counterpropagating configuration is employed.

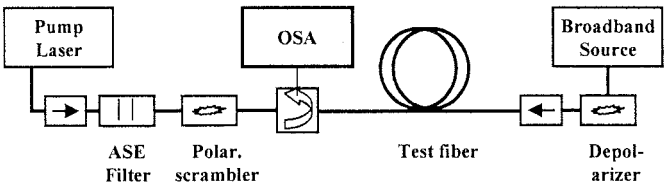

Fig. 1. Schematic of the experimental setup to measure Raman gain with a high-power pump laser.

For these measurements, we used pump diodes at both 1450 and 1490 nm that provide about 30 mW of launched pump power into the fiber under test. The "signal" is provided by a ~ 30 μW broadband source that covers the spectral range from 1.25 to 1.7 μm and is depolarized by a passive Lyot depolarizer. A circulator at the fiber output directs the signal light to an optical spectrum analyzer for analysis. Based on the broadband power spectrum, the modulation of the pump laser by the probe source is estimated to be $< 10^{-4}$, so that the undepleted pump approximation is well satisfied. In order to remove the effects of spontaneous Raman scattering from the laser, three OSA scans are taken: one with just the broadband source on, denoted $S_{\rm off}(\lambda)$; one with both the broadband source and laser on, denoted $S_{\rm on}(\lambda)$; and one with just the laser on, denoted $S_{\rm laser}(\lambda)$. The modal Raman gain spectrum is then calculated as

$$g(\Delta\omega) = \frac{1}{P_p L_{\rm eff}} \ln\left(\frac{S_{\rm on} - S_{\rm laser}}{S_{\rm off}}\right) \tag{13}$$

where the effective length is defined in terms of the attenuation constant at the pump wavelength α and the fiber length L, as $L_{\rm eff} = (1 - \exp(-\alpha L))/\alpha$. The launched pump power P_p is determined by correcting the measured power exiting the fiber-under-test for the splice loss at the fiber end (from splicing on a connector) and for the fiber attenuation, which is measured by the cutback method.

The absolute uncertainty in the gain strength is $\sim$1.8% and depends primarily on the uncertainty in the pump power and fiber attenuation. The relevant uncertainty for the gain-comparison method is the relative uncertainty in the gain strength at different pump wavelengths; this uncertainty is estimated to be

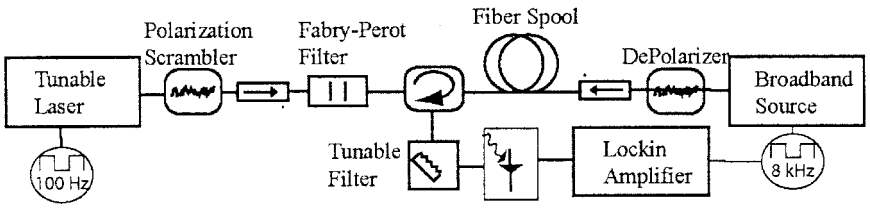

Fig. 2. Schematic of the experimental setup for measuring Raman gain with a low-power pump laser.

$\sim$1%, and, as is shown in Table I, translates to a much larger uncertainty in the power-law exponent that describes the pump-wavelength scaling.

Unlike the gain-comparison method, the gain-asymmetry method is completely independent of the uncertainty in the absolute strength of the gain since it uses (6) to determine the pump-wavelength scaling. The gain-asymmetry method, however, is sensitive to uncertainty in the shape of the Raman gain spectrum. A number of precautions discussed above are taken to minimize systematic changes in the shape of the gain curve. There are two main additional contributions: power drift of the broadband probe source and relative wavelength uncertainty of the pump and spectrally resolved probe light. Power drifts in the probe source are mitigated by acquiring several successive Raman gain measurements with the OSA using two different ordering of the scans: $S_{\rm on}(\lambda) \rightarrow S_{\rm off}(\lambda) \rightarrow S_{\rm laser}(\lambda)$ and $S_{\rm laser}(\lambda) \rightarrow S_{\rm off}(\lambda) \rightarrow S_{\rm on}(\lambda)$. The average Raman gain from these runs is much less sensitive to systematic drifts induced by turning off or on the broadband source (a fiber switch is used to turn the pump laser on or off so that its output power is much more stable). Any residual effects of slow drifts of the probe power are estimated directly from the data in the following fashion. For a given run, the set of traces are labeled $S^i_{\rm on}(\lambda)$ (or $S^i_{\rm off}(\lambda)$), where i denotes a single scan within a larger set of scans. A spurious drift-induced Raman gain is calculated from the average of the quantity $\ln[S^i_{\rm on}(\lambda)/S^{i\pm1}_{\rm on}(\lambda)]$ over all the traces in the particular set. This spurious gain is added to the real Raman gain and the asymmetry is recalculated to determine the resulting uncertainty in the power-law scaling. For a set of 18 runs, the effects of the slow drifts are typically smaller than those of the wavelength uncertainty, discussed next. The effects of slow drifts in the probe would, of course, be even less significant if a pump laser of higher power were used.

The relative wavelength uncertainty between the pump and spectrally resolved probe light is estimated to be $\pm$0.1 nm (or $\sim$12.5 GHz) based on uncertainty in the estimated line center of the pump laser and the OSA used in this experiment. From (4), this wavelength uncertainty translates to an uncertainty in the asymmetry. The effect of this wavelength uncertainty is estimated by recalculating the asymmetry (4) after shifting $\Delta\omega$ by $\pm$12.5 GHz; the resulting spread in the values for the power-law exponent n_s is taken as the uncertainty in n_s. The effect of the wavelength uncertainty on the uncertainty in n_s depends on the full useful range of $\Delta\omega$; the smaller the range in $\Delta\omega$ over which the asymmetry is calculated, the larger the effect of the 12.5-GHz uncertainty. Since the useful range in $\Delta\omega$ is determined by the wavelength-dependent fiber attenuation (due to attenuation of the probe signal), the uncertainty in n_s that results from the wavelength uncertainty will depend on the fiber attenuation and therefore the fiber type. The relative contribution to the total uncertainty for the gain-asymmetry method, given in Table I and Fig. 9, is dominated by the wavelength uncertainty, followed by the uncertainty from the probe power drift, and finally by random statistical uncertainty.

C. Experimental Setup for a Low-Power Pump Laser

The above experimental setup works well, provided that the induced Raman gain on the signal is large enough that the slow drifts in the probe power and OSA response are indeed much smaller than the gain that is being measured. If the pump power is low, the gain may be too low for an accurate measurement, and an alternative experimental setup is needed. There are several potential situations in which only a low-power pump might be available. For example, in [17], the author wanted to have a full set of spectra at different pump wavelengths in order to compare the gain-comparison method to the gain-asymmetry method of measuring the pump-wavelength scaling; a tunable laser was chosen to avoid the otherwise cumbersome and expensive proposition of operating multiple high-power pumps at different wavelengths. As another example, the gain-asymmetry method provides only an approximate pump-wavelength dependence for the Raman gain in DCF fiber; direct measurements at the pump-wavelength of interest are needed for an accurate description. A high-power pump may not always be available for the wavelength of interest, particularly within the signal band where the Raman gain is needed to determine the effects of Raman gain tilt. Reference [17] described one potential setup that permits measurement of accurate Raman gain profiles with a tunable pump laser of very low power. Here we briefly summarize that setup.

The basic experimental configuration is shown in Fig. 2. An external cavity laser, tunable over the range of 1460–1580 nm, serves as the pump source. As with the previous setup, the pump is filtered to remove ASE, and its polarization is scrambled. The total launched power ranges from 2 to 5 mW, depending on the wavelength. The resulting typical peak Raman gain ($\sim$100 nm from the pump laser) is only about 2×10^{-2}. At a wavelength offset of 5 nm from the pump laser, this gain drops to 1×10^{-3}. A measurement at the 1% level at low wavelength offsets therefore requires measuring the signal gain at levels as low as 10 ppm, which requires low statistical and systematic uncertainties. To achieve this high sensitivity, a double modulation technique is employed. The laser output is amplitude-modulated by a 100-Hz square wave and transmitted down the fiber-under-test. The broadband source (identical to the one previously described) is similarly amplitude-modulated by an 8-kHz square wave and launched down the fiber in the opposite direction. At

the end of the fiber, the broadband probe light is redirected by a circulator to a 1/8-m grating monochromator that serves as a tunable optical filter with a full-width half-maximum of 1.75 nm. The filtered output of the monochromator is coupled into a multimode fiber and detected by a PIN diode followed by a transimpedance amplifier and a lock-in amplifier, which detects the amplitude of the 8-kHz probe signal. The lock-in output provides $S_{\rm on}(\lambda) - S_{\rm laser}(\lambda)$ when the laser is modulated on and $S_{\rm off}(\lambda)$ when the laser is modulated off. The gain is calculated again from (13). The underlying measurement is exactly the same as that described above for a high-power laser; however, by modulating the signal and pump, the "$1/f$" noise on both the probe power and detector response is greatly reduced, with a corresponding increase in sensitivity for the Raman gain.

As with the simpler setup, the overall uncertainty in the absolute Raman gain was about 1.8%, resulting from uncertainties in the pump power and in the fiber attenuation. For the gain-comparison method, the uncertainty in the power-law scaling exponent is determined from the relative uncertainty in the gain from one pump wavelength to the next pump wavelength, which was estimated to be 1% for these data.

Again, for the gain-asymmetry method, the uncertainty in the absolute gain is irrelevant; only uncertainties in the shape of the gain matter. A potentially troublesome polarization effect, which can distort the shape, is nonlinear polarization rotation [5] of the probe, which, when combined with a polarization-dependent response (PDR) of the monochromator, mimics Raman gain. However, the low relative polarization of the pump and signal reduces this effect to $< 2 \times 10^{-4}$ of the peak Raman gain. (This effect is not present for the OSA-based measurement because of the very low PDR of the OSA.) The point-to-point uncertainty in the Raman gain curve was on the order of 0.5% or less across the spectrum, including both this PDR effect and statistical uncertainties. As before, the dominant uncertainty in the measurements of the pump-wavelength scaling using the gain-asymmetry approach resulted from uncertainty in the wavelength calibration. The monochromator filter was cross-calibrated with an OSA that had been previously calibrated with a hydrogen cyanide reference and free-space etalon. The uncertainty in the relative wavelength calibration between the pump laser and the filtered broadband source was estimated to be ± 0.2 nm over the wavelength range of interest.

V. Gain-Asymmetry and Gain-Comparison Methods: Results and Discussion

The wavelength dependence of the Raman gain was measured using both techniques discussed above for a number of different transmission fibers with $\sim$25 km lengths at a range of pump wavelengths. Table I summarizes the results of all the measurements. Before discussing these results, however, we discuss some representative data and the analysis used to determine the pump-wavelength scaling.

A. Raman Gain Spectra

Fig. 3 shows the full Raman gain spectrum for a series of fibers taken at 1480 nm using the setup of Fig. 1. Fig. 4 shows the Raman gain for one fiber at a series of different pump wavelengths taken with the setup of Fig. 2. The basic trends are clear in the data of Figs. 3 and 4. The Raman gain strength decreases with increasing pump wavelength. There is a corresponding strong asymmetry such that the anti-Stokes loss is larger than the Stokes gain—i.e., the probe light at shorter wavelengths—loses more energy pumping the pump laser than the pump laser transfers to the longer wavelength probe light. The Raman gain is, as expected, considerably higher for fibers with smaller effective areas, e.g., DCF, LEAF, and TrueWave, than for SMF-28. Finally, the similar fiber types have very similar Raman gain spectra.

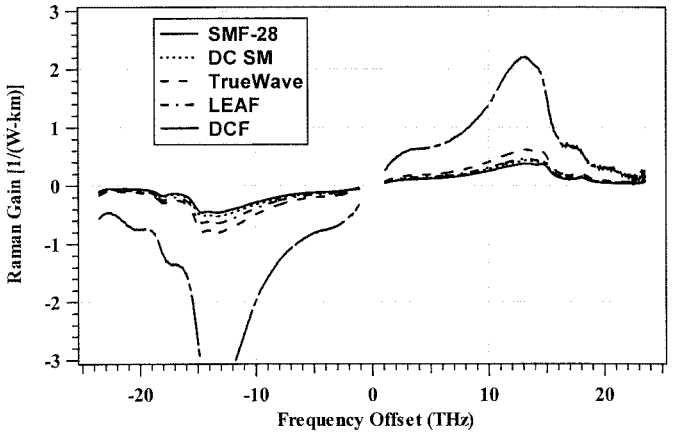

Fig. 3. Full Raman gain spectrum for five different fibers at a pump wavelength of 1480 nm measured with a high-power pump laser and the setup of Fig. 1.

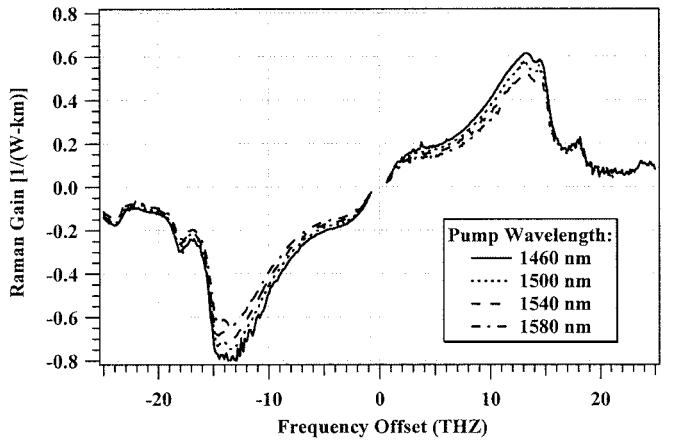

Fig. 4. Full Raman gain spectrum for TrueWave fiber measured using a low-power pump laser and the setup of Fig. 2.

B. Gain-Comparison Method

As discussed earlier, the pump-wavelength dependence of the Raman gain can be extracted from these data in two different, complementary ways: from a comparison of the gain strength or from the gain asymmetry. To calculate the wavelength dependence using the gain-comparison approach, the integrated Raman gains for different pump wavelengths are plotted versus wavelength on a log–log plot, and a straight line is fitted to the data (see Fig. 5). The overall uncertainty in determining the power-law scaling exponent n_s depends on the uncertainty assigned to the integrated gain values. For the data of Fig. 6, the

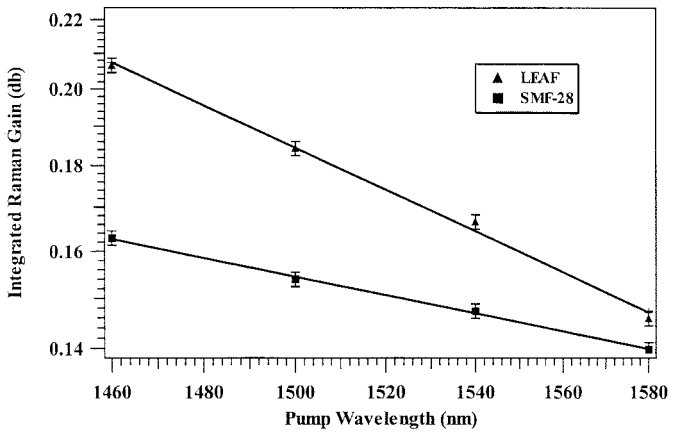

Fig. 5. Integrated Raman gain as a function of pump wavelength for LEAF fiber (solid triangles) and SMF-28 (squares). The solid line is a fit to the data; its slope gives the power-law scaling exponent for the pump-wavelength scaling of the Raman gain by use of the gain-comparison method.

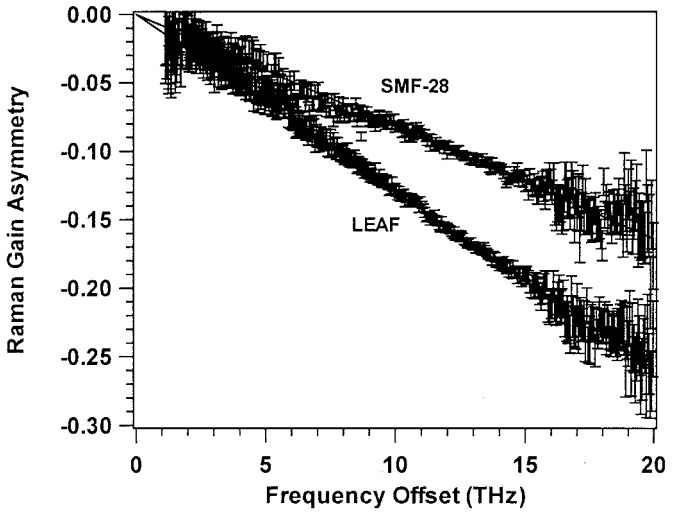

Fig. 6. Asymmetry in the Raman gain for SMF-28 fiber (shallower slope) and LEAF fiber (steeper slope). These curves are derived directly from a single Raman gain spectrum at a pump wavelength of 1480 nm (from the data of Fig. 4). The slope yields the power-law pump-wavelength scaling of the Raman gain.

relative uncertainty in the gain over the range of pump wavelengths from 1460 to 1580 nm was estimated to be 1%, resulting in an overall uncertainty for n_s of ± 0.17 (see the top of Table I). For similar data taken with only two high-power pumps using the setup of Fig. 1, the same relative uncertainty of 1% leads to an even higher uncertainty in n_s of ± 0.68 (see bottom of Table I) since there are only two more closely spaced pump wavelengths of 1450 and 1480 nm.

The gain-comparison method was also used in [28] to determine the power-law scaling of the Raman gain. In that work, they found a power-law exponent of $n_s = 5.1 \pm 1$ for LEAF fiber and $n_s = 3.5 \pm 0.7$ for TrueWave fiber, in good agreement with the values of Table I.

C. Gain-Asymmetry Method

The gain-asymmetry approach extracts the wavelength dependence directly from the asymmetry in the Raman gain curves following (6). An example of the asymmetry calculated from

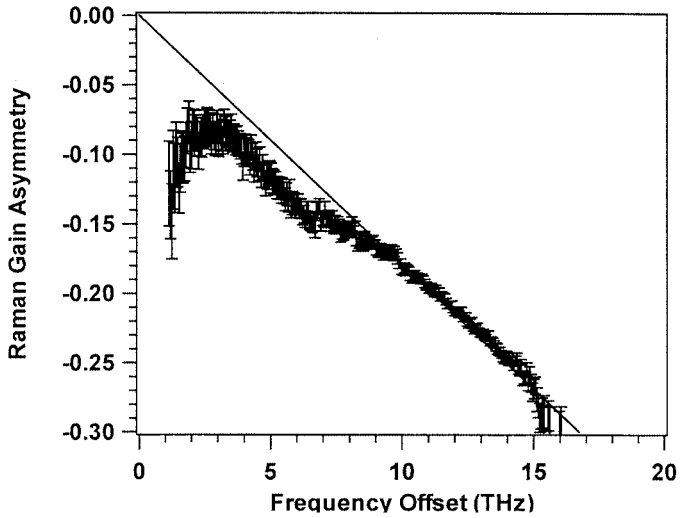

Fig. 7. Asymmetry in the Raman gain for DCF based on the Raman gain spectrum shown in Fig. 3. The asymmetry diverges substantially from a straight line, indicating that its dependence on pump wavelength is not well described as a simple scaling law.

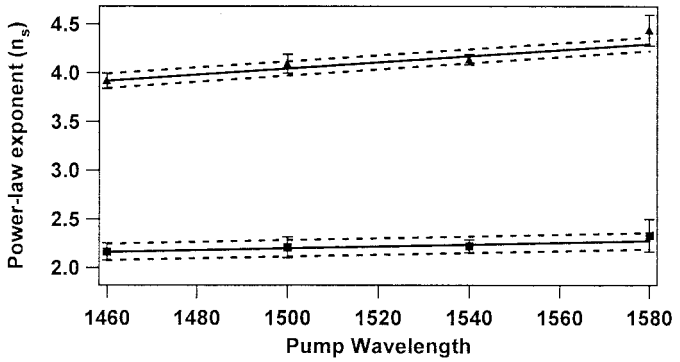

Fig. 8. Exponent for power-law scaling of the pump-wavelength dependence of the Raman gain for LEAF (solid triangles) and SMF-28 (solid squares) fiber as a function of the pump wavelength. Each point was calculated from the slope of the gain asymmetry, which was calculated in turn from the Raman gain curve at each pump wavelength (as in Fig. 7). The solid line is a fit to the data. The error bar on each point includes the uncertainty in the relative pump-signal wavelength of 0.2 nm, half of which is taken as uncorrelated between data points and half as correlated; the dashed lines represent the effect of the correlated wavelength uncertainty.

these curves for different fiber types is given in Fig. 6. Near zero, the asymmetry sometimes diverges slightly from a straight line due to the combined effect of small residual stray light and uncertainties in the relative pump and probe wavelengths, which result in a stronger effect at small wavelength offsets. The scaling of the Raman gain is determined by a straight-line fit to the asymmetry, the slope of which gives the power-law scaling exponent $n_s(\lambda_p)$ for a given pump wavelength. Unlike the gain-comparison method, the gain-asymmetry method yields a value of the power-law scaling exponent from a single Raman gain curve.

The basic assumption of separability in (2), inherent in discussing the pump-wavelength scaling of the Raman gain curve, is verified by the excellent fit of the data of Fig. 6 to a straight line. This behavior is observed for all the fibers examined, except for the DCF fiber. The gain asymmetry for the DCF fiber diverges considerably from a straight line, as is shown in Fig. 7.

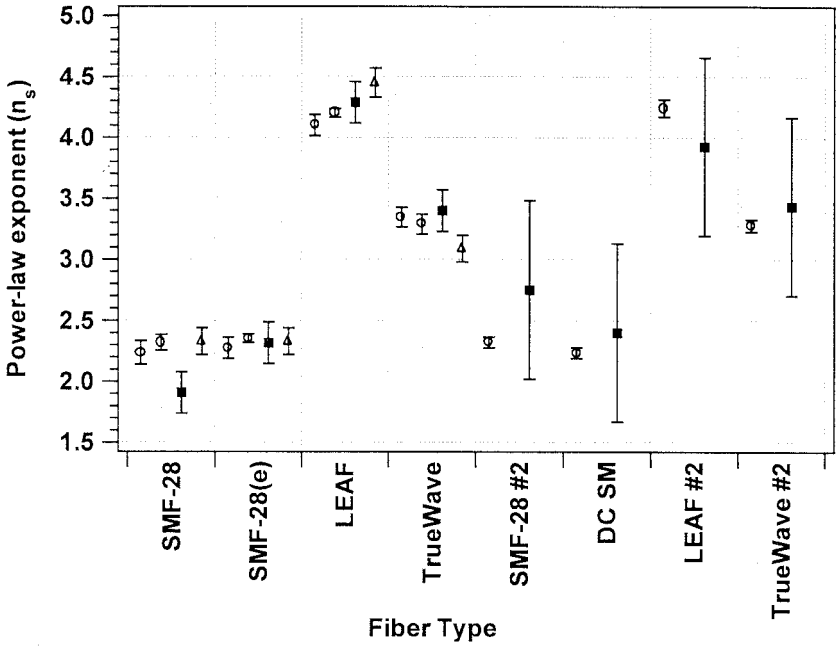

Fig. 9. Summary of the data in Table I. The circles represent measurements using the gain-asymmetry method, the squares represent measurements using the gain-comparison method, and the triangles represent estimates from theory and known fiber parameters. The uncertainties are all at the 1-sigma level.

The reason for this divergence is that the magnitude and *shape* of the Raman gain vary with pump wavelength; the assumption of separability is violated. Note that this effect can also be observed by simply plotting the ratio of the Raman gain at one pump wavelength to the Raman gain at a different pump wavelength; this ratio will not be a straight line, which indicates again that the shape of the Raman gain curve changes with pump wavelength. Therefore, it is impossible to extract a complete description of the Raman gain at a particular pump wavelength from measurements at different pump wavelengths. However, it is still true that the Raman loss at a signal wavelength offset $\delta\lambda$ below the pump wavelength λ_0 permits an accurate prediction of the Raman gain for a pump at a wavelength of $\lambda_0-\delta\lambda$ and signal at a wavelength of λ_0. Note that this breakdown of the simple scaling of the Raman gain is a basic feature of the DCF fiber and is not related to whether the measurement is made using the gain-asymmetry method or the gain-comparison method.

Since the gain-asymmetry method provides an estimate of the power-law scaling of the pump-wavelength dependence at each pump wavelength, we can explore the variation of the power-law dependence with wavelength. In other words, we can let the exponent n_s vary with pump wavelength. Fig. 8 shows the values of n_s at each wavelength and a fit of these data to a straight line to find the dependence of the exponent on pump wavelength $dn_s/d\lambda$ (a quantity not available using the integrated gain strength at each pump wavelength because of the larger uncertainties and few effective data points). Values for the slope of the power-law exponent are given in Table II for several fiber types.

The advantage of the gain-asymmetry method is that the uncertainties can be significantly smaller than the gain-comparison method, which relies on the relative power measurements. The improved uncertainty is evident in Table I and is even more obvious in Fig. 9, which summarizes the results graphically. Clearly the gain-asymmetry method provides a smaller uncertainty than either the gain-comparison method or estimates from theory.

VI. Effect on Distributed Raman Amplification

The ultimate amplification in a distributed Raman amplifier will depend on both the Raman gain coefficient, discussed in detail above, and the fiber attenuation at the pump wavelength (which is not included in (1) for simplicity). For a fiber length $L \gg L_{\text{eff}}$, the overall on/off Raman amplification of the signal is given from (13) by $G = \exp(P_p g^{+}(\Delta\omega)/\alpha)$, where α is the attenuation at the pump wavelength. Therefore, the overall pump-wavelength dependence of the gain G will depend on the pump-wavelength dependence of *both* the Raman gain g and the fiber attenuation. For the fibers and wavelength ranges considered here, the attenuation at the pump wavelengths will be dominated by the tail of the weak water peak at 1.39 μm. We measure a dependence from 1450 to 1500 nm of $\alpha \sim \omega_p^{3.5}$ for SMF-28, SMF-28e, and LEAF fibers and $\alpha \sim \omega_p^{5.5}$ for TrueWave fiber. This wavelength dependence effectively *counters* the wavelength dependence of the Raman gain coefficient of Table I. As a result, the overall on/off Raman gain in a distributed amplifier will actually increase with increasing pump wavelength for all but LEAF fiber. In other words, although the Raman gain coefficient increases with decreasing wavelength, the increased attenuation of the pump at decreasing wavelengths leads to a reduction in the overall Raman gain with decreasing wavelengths for most fibers.

VII. Conclusion

The Raman gain in single-mode fiber will depend on both the signal and pump wavelengths. This dependence is most easily discussed in terms of a Raman gain curve that depends only on

the pump-signal wavelength or frequency offset, and an overall scaling factor that depends on the pump wavelength. We present three possible methods for determining the scaling of the Raman gain with pump wavelength. The gain-asymmetry method provides the pump-wavelength scaling directly with the least uncertainty and effort. Knowledge of the pump-wavelength scaling of the Raman gain should assist in the simulation and design of Raman amplifiers using many pump lasers to flatten the gain, the determination of the effect of Raman gain tilt in WDM systems, and simulation of other Raman-based effects. Finally, if the contribution from the matrix element to the scaling is subtracted from the overall power-law scaling, this measurement can also provide a reasonable estimate of the wavelength scaling of the effective area, a quantity that is important in many nonlinear effects.

ACKNOWLEDGMENT

The author thanks S. Gilbert and K. Corwin for useful discussions. The author also thanks the participants of the TIA Raman gain round-robin measurement for providing some of the fibers used in these measurements.

REFERENCES

[1] R. H. Stolen and E. P. Ippen, "Raman gain in glass optical waveguides," *Appl. Phys. Lett.*, vol. 22, pp. 276–278, 1973.
[2] D. Marcuse, *Principles of Quantum Electronics*. New York: Academic, 1980.
[3] Y. R. Shen, *The Principles of Nonlinear Optics*. New York: Wiley, 1984.
[4] Y. Aoki, "Properties of fiber Raman amplifiers and their applicability to digitial optical communication systems," *J. Lighwave Technol.*, vol. 6, pp. 1225–1239, 1988.
[5] G. P. Agrawal, *Nonlinear Fiber Optics*, 2nd ed. New York: Academic, 1995.
[6] Y. Emori, K. Tanaka, and S. Namiki, "100 nm bandwidth flat-gain Raman amplifiers pumped and gain equalized by 12-wavelength-channel WDM laser diode unit," *Electron. Lett.*, vol. 35, pp. 1355–1356, 1999.
[7] K. Rottwitt and H. D. Kidorf, "A 92-nm bandwidth Raman amplifier," in *Optical Fiber Communication Conf. 1998*, 1998, p. PD6.
[8] D. J. Dougherty, F. X. Kartner, H. A. Haus, and E. P. Ippen, "Measurement of the Raman gain spectrum of optical fibers," *Opt. Lett.*, vol. 20, p. 31, 1995.
[9] S. Gray, "Raman gain measurements in optical fibers," in *Symp. Optical Fiber Measurements*, G. W. Day, D. L. Franzen, and P. A. Williams, Eds., 2000, NIST Special Publication 953, p. 151.
[10] D. Hamoir, N. Torabi, A. Bergonzo, S. Borne, and D. Bayart, "Raman spectra of line fibers measured over 30 THz," in *Symp. Optical Fiber Measurements*, G. W. Day, D. L. Franzen, and P. A. Williams, Eds., 2000, NIST Special Publication 953, p. 147.
[11] F. Koch, S. A. E. Lewis, S. V. Chernikov, and J. R. Taylor, "Broadband Raman gain characterization in various optical fibers," *Electron. Lett.*, vol. 37, p. 1437, 2001.
[12] S. A. E. Lewis, S. V. Chernikov, and J. R. Taylor, "Temperature-dependent gain and noise in fiber Raman amplifiers," *Opt. Lett.*, vol. 24, pp. 1823–1825, 1999.
[13] D. Mahgerefteh, D. L. Butler, J. Goldhar, B. Rosenberg, and G. L. Burdge, "Technique for measurement of the Raman gain coefficient in optical fibers," *Opt. Lett.*, vol. 21, p. 2026, 1996.
[14] P. B. Hansen, A. J. Stentz, and T. N. Nielson, "Raman applications in optical transmission systems," in *Trends in Optics and Photonics (TOPS)*, A. Mecozzi, M. Shimizu, and J. Zyskind, Eds. Washington, DC: Optical Society of America, 2002, vol. 44, Optical Amplifiers and their Applications, p. 18.
[15] C. Fludger, A. Maroney, N. Jolley, and R. Mears, "An analysis of the improvements in OSNR from distributed Raman amplifiers using modern transmission fibers," in *Optical Fiber Communication Conf.*, 2000, p. FF2.
[16] F. Boubal, E. Brandon, L. Buet, V. Havard, P. L. Rouz, L. Labrunie, L. Piriou, and J.-P. Blondel, "Raman amplification in unrepeatered submarine systems pushes the limits of distance and bandwidth," in *Trends in Optics and Photonics (TOPS)*. Washington, DC: Optical Society of America, 2002, vol. TOPS 77, Optical Amplifiers and their Applications, p. OMA2-1.
[17] N. R. Newbury, "Raman gain: Pump-wavelength dependence in single-mode fiber," *Opt. Lett.*, vol. 27, p. 1232, 2002.
[18] N. R. Newbury and K. L. Corwin, "Comparison of stimulated and spontaneous scattering measurements of the full wavelength dependence of the Raman gain spectrum," in *Symp. Optical Fiber Measurements*, G. W. Day, D. L. Franzen, and P. A. Williams, Eds., 2002, NIST Special Publication 988, p. 7.
[19] N. R. Newbury, "Pump wavelength dependence of Raman gain," in *Trends in Optics and Photonics (TOPS)*, vol. 77, Optical Amplifiers and their Applications, Washington, DC, 2002, p. OME9.
[20] K. Rottwitt, J. Bromage, M. Du, and A. Stentz, "Design of distributed Raman amplifiers," presented at the ECOC'2000, Munich, Germany, 2000.
[21] C. R. S. Fludger, V. Handerek, and R. J. Mears, "Fundamental noise limits in broadband Raman amplifiers," in *OSA Trends in Optics and Photonics Series (TOPS)*, vol. 54, Optical Fiber Communication Conference, Washington, DC, 2001, p. MA5-1.
[22] F. L. Galeener, J. C. Mikkelsen, R. H. Geils, and W. J. Mosby, "The relative Raman cross sections of vitreous SiO_2, GeO_3, B_2O_3, and P_2O_5," *Appl. Phys. Lett.*, vol. 32, pp. 34–36, 1978.
[23] S. T. Davey, D. L. Williams, B. J. Ainslie, W. J. M. Rothwell, and B. Wakefield, "Optical gain spectrum of GeO_2-SiO_2 Raman fiber amplifiers," in *Proc. Inst. Elect. Eng.*, vol. 136, 1989, p. 301.
[24] J. Bromage, K. Rottwitt, and M. E. Lines, "A method to predict the Raman gain spectrum of germanosilicate fibers with arbitrary index profiles," *IEEE Photon. Technol. Lett.*, vol. 14, p. 24, 2002.
[25] R. H. Stolen, "Issues in Raman gain measurements," in *Symp. Optical Fiber Measurements 2000*, NIST Special Pub. 953, P. A. Williams and G. W. Day, Eds., 2000, p. 146.
[26] Y. Namihira, "Wavelength dependence of correction factor of effective area and mode field diameter in various optical fibers," in *Symp. Optical Fiber Measurements*, NIST Special Pub. 953, G. W. Day, D. L. Franzen, and P. A. Williams, Eds., 2000.
[27] D. A. Humphreys, R. S. Billington, A. Parker, B. Walker, D. S. Wells, A. G. Hallam, and I. Bongrand, "A comparison of three techniques for effective area measurement of single-mode optical fibers," in *Symp. Optical Fiber Measurements*, G. W. Day, D. L. Franzen, and P. A. Williams, Eds., 2000, NIST Special Publication 953, p. 61.
[28] K. J. Cordina and C. R. S. Fludger, "Changes in Raman gain coefficient with pump wavelength in modern transmission fibers," in *Trends in Optics and Photonics (TOPS)*. Washington, DC: Optical Society of America, 2002, vol. 77, Optical Amplifiers and their Applications, p. OMC3.
[29] "Continuous wave method for measuring the Raman gain efficiency of single-mode fibers," Telecommunications Industry Association, Arlington, VA, TIA/EIA-TSB-62–22, 2001.
[30] Q. Lin and G. P. Agrawal, "Polarization mode dispersion-induced fluctuations during Raman amplification in optical fibers," *Opt. Lett.*, vol. 27, pp. 2194–2196, 2002.
[31] C. R. S. Fludger, V. Handerek, and R. J. Mears, "Pump to signal RIN transfer in Raman fiber amplifiers," *J. Lightwave Technol.*, vol. 19, pp. 1140–1148, 2001.

Nathan R. Newbury received the B.A. degree in physics from Williams College, Williamstown, MA, in 1986 and the Ph.D. degree in physics from Princeton University, Princeton, NJ, in 1992.

He was a Postdoctoral Associate with C. Wieman working toward the production of Bose–Einstein condensation in laser cooled atoms. He then joined the Massachusetts Institute of Technology Lincoln Laboratory in 1996, where he worked in a number of areas, including biodetection and LIDAR. In 2001, he joined the Fiber Optics and Components Group, Optoelectronics Division, National Institute of Standards and Technology, where he is currently working in the area of nonlinear fiber optics.